Computational Modelling of Radar Interaction and Return from Overdense Meteor Trails

Sohaib Haq

College of Natural Science & Mathematics, University of Alaska Fairbanks

EE 488: Undergraduate Research / PHYS 400: Capstone Project

Professor Denise Thorsen

Professor Martin Truffer

Abstract

Meteor radars study Earth's mesosphere by reflecting electromagnetic waves in the radio wavelength off ionized meteor trails. Data from meteor radars stationed at University of Alaska Fairbanks (UAF) Poker Flats Research Range (PFRR) showed unexpected oscillations in the decay scheme of the return signal from overdense meteor trails. It is hypothesized that these oscillations may be the result of Mie scattering, a scattering regime where an object's radar cross-section (RCS) is dependent on the object's circumference relative to the incident radiation wavelength, occurring as the meteor trail expands. In an effort to better understand the phenomenon, this project offers EMITRACK: a finite-difference time-domain (FDTD) model of electromagnetic waves interacting with an approximation of the meteor trail. By solving Maxwell's equations using finite difference approximations of the derivative across a staggard Yee grid and by approximating an overdense meteor trail as an infinitely extruded cylindrical perfect electric conductor (PEC), a model of the relevant interaction was produced. This model is currently incomplete and requires an implementation of a near-field to far-field transform and total field/scatter field boundaries surrounding the grid. This report includes an introduction to the FDTD method, implementation details in EMITRACK, and the tests conducted to determine the validity and function of the model in its current state. This report briefly discusses steps to be taken by future researchers to further refine the program. The EMITRACK program can be found on GitHub at https://github.com/raptor287/emitrack.

Introduction

Meteors are small chunks of space debris, typically around the size of a grain of rice, that enter Earth's atmosphere at speeds ranging from 11 km/s to 71 km/s (Richardson & Bedient, n.d.). The meteors experience collisions with atmospheric gas particles wherein the energy transferred from the meteor causes the gas particles to be ionized; the outer electrons of the gas molecules are stripped away. The net effect of this interaction is a trail of plasma spanning tens of kilometers (Manning, Villard, & Peterson, 1952) at altitudes ranging from 70 km to 100 km (Baggaley & Fisher, 1978). Since plasma is a sea of free electrons, it makes for an excellent reflector of electromagnetic waves. By emitting a radio wave towards the plasma trail from a ground-based radar emitter; recording the subsequent reflected signal; and analyzing the signal as a function of altitude, researchers can determine properties of Earth’s atmosphere without the need for costly rockets carrying probing equipment (Wislez, 1996). This data gives valuable information to include atmospheric winds at high altitudes which can be used to determine heat transfer across the planet.

University of Alaska Fairbanks utilizes this methodology with radar arrays stationed at the Poker Flats Research Range. These radars emit waves at a central frequency of 32.55 MHz using a shaped amplitude profile with a width of 5 μs at a pulse repetition frequency of 625 Hz. Data collected from these radars showed unexpected oscillations in the return signal decay from an overdense meteor (Figure 7). It is hypothesized that these oscillations are the result of Mie scattering: a phenomenon where a spherical scatterer’s radar cross-section oscillates as a function of the ratio of the incident wavelength and the circumference of the object when the ratio is near

1. Assuming this holds true for cylindrical scatterers, it may be possible for the meteor trail to pass through Mie scattering regimes as the trail expands radially.

To further understand the interaction between radio waves and overdense meteor trails, this project offers EMITRACK: a finite-difference time-domain (FDTD) model of electromagnetic waves interacting with a perfectly conducting cylinder of variable radius programmed in the Python language. By modelling the interaction between EM waves in the radio wavelengths interacting with the PEC cylinder in polarizations both normal and parallel to the cylinder's z-axis, researchers can visualize the event and gain further insight into the phenomena.

Methodology

Finite Difference Time Domain (FDTD)

Finite-difference time-domain is a numerical method of solving Maxwell's equations first introduced by Kane Yee in 1966 (Wikipedia, 2022). FDTD uses central finite difference approximations of each vector component of the electric and magnetic field in Maxwell's curl equations across a staggard "Yee" grid. These finite difference equations are then solved inside a loop iterating over time. The equations ultimately provide the electric and magnetic fields at discrete points in time and space. This method is widely used in computational electrodynamics to simulate EM waves and provides a computationally cheap, robust, and intuitive solution to Maxwell's equations (Rumpf, n.d.).

Brief Introduction to Maxwell's Equations.

Maxwell's equations are a set of four partial differential equations that describe the behavior of electric and magnetic fields through time and space. These equations can be categorized into two divergence equations:

Gauss' Law: $$\vec{\nabla} \cdot \vec{E} = \frac{\rho}{\epsilon_0}$$

Gauss' Law for Magnetism: $\vec{\nabla} \cdot \vec{B} = 0$

where $\vec{\mathbf{E}}$ is the electric field; $\boldsymbol{\rho}$ is a charge density; $\boldsymbol{\epsilon_0}$ is the free space permittivity constant; and $\vec{\boldsymbol{B}}$ is the magnetic field, and two curl equations:

Faraday's Law: $\vec{\nabla} \times \vec{E} = -\frac{\partial \vec{B}}{\partial t}$

Ampere's Law[1]: $\vec{\nabla} \times \vec{B} = \mu_0 \left(\vec{J} + \epsilon_0 \frac{\partial \vec{E}}{\partial t} \right)$

where $\boldsymbol{\mu_0}$ is the free space permeability constant and $\vec{\boldsymbol{J}}$ is an electric current density.

The divergence equations describe the sources of electric and magnetic fields. The electric field source is a charge distribution $\boldsymbol{\rho}$ and the magnetic field has no sources and consequently creates loops. The curl equations describe the rotating electric fields induced by a time changing magnetic field in the case of Faraday's law and vice-versa in the case of Ampere's law. Together, the curl equations predict electromagnetic waves and their propagation through time and space. Therefore, by solving Maxwell's equations, electromagnetic waves and their interaction with material can be described.

The Yee Grid.

Prior development into numerical methods for solving PDEs have shown that second order accuracy may be achieved through staggering finite difference operators in time and space. In his 1966 paper, Kane Yee applied these concepts to the curl operators in Maxwell's equations (Wikipedia, 2022). This was done by defining electric field quantities

[1]More precisely, Ampere's Law with Maxwell's correction.

to exist at integer spatial and temporal positions and magnetic field quantities to exist at positions halfway between the electric field quantities.

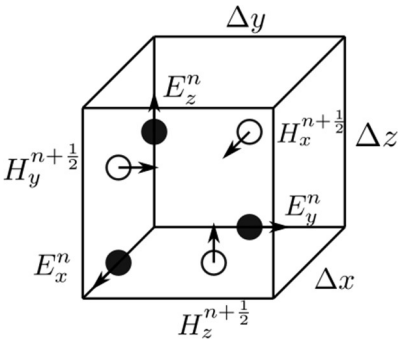

Figure 1. The image to the right shows magnetic field quantities staggard by a half cell from the electric fields.

Source: File:Yee cell.png - https://en.wikipedia.org

The use of this staggard Yee grid also conveniently satisfies Maxwell's divergence equations as well as boundary conditions at changing media.

When programming, the temporal stagger enters implicitly through the placement of update equations in the time loop. When the magnetic field update equation appears first, it is effectively being updated every half time step with intervals of a whole time step. Consequently, the electric field is updated every whole time step.

FDTD Basic Update Equations.

To derive the update equations for the electric and magnetic fields, one of the fields is normalized by multiplying the free space impedance and the curl operations in Maxwell's equations are expanded:

$$\frac{\partial E_z}{\partial y} - \frac{\partial E_y}{\partial z} = -\frac{\mu_{xx}}{c_0}\frac{\partial \widetilde{H_x}}{\partial t} \qquad \frac{\partial \widetilde{H_z}}{\partial y} - \frac{\partial \widetilde{H_y}}{\partial z} = \frac{\epsilon_{xx}}{c_0}\frac{\partial E_x}{\partial t}$$

$$\frac{\partial E_x}{\partial z} - \frac{\partial E_z}{\partial x} = -\frac{\mu_{yy}}{c_0}\frac{\partial \widetilde{H_y}}{\partial t} \qquad \frac{\partial \widetilde{H_x}}{\partial z} - \frac{\partial \widetilde{H_z}}{\partial x} = \frac{\epsilon_{yy}}{c_0}\frac{\partial E_y}{\partial t}$$

$$\frac{\partial E_y}{\partial x} - \frac{\partial E_x}{\partial y} = -\frac{\mu_{zz}}{c_0}\frac{\partial \widetilde{H_z}}{\partial t} \qquad \frac{\partial \widetilde{H_y}}{\partial x} - \frac{\partial \widetilde{H_x}}{\partial y} = \frac{\epsilon_{zz}}{c_0}\frac{\partial E_z}{\partial t}$$

In this case, the magnetic field ***H*** was normalized. These equations are then discretized using finite difference approximations. The discretized equations must be such that all elements exist at the same point in time and space:

$$\frac{E_z^{i,j+1,k}|_t - E_z^{i,j,k}|_t}{\Delta y} - \frac{E_y^{i,j,k+1}|_t - E_y^{i,j,k}|_t}{\Delta z} = -\frac{\mu_{xx}^{i,j,k}}{c_0}\frac{\widetilde{H}_x^{i,j,k}|_{t+\frac{\Delta t}{2}} - \widetilde{H}_x^{i,j,k}|_{t-\frac{\Delta t}{2}}}{\Delta t}$$

$$\frac{E_x^{i,j,k+1}|_t - E_x^{i,j,k}|_t}{\Delta z} - \frac{E_z^{i+1,j,k}|_t - E_z^{i,j,k}|_t}{\Delta x} = -\frac{\mu_{yy}^{i,j,k}}{c_0}\frac{\widetilde{H}_y^{i,j,k}|_{t+\frac{\Delta t}{2}} - \widetilde{H}_y^{i,j,k}|_{t-\frac{\Delta t}{2}}}{\Delta t}$$

$$\frac{E_y^{i+1,j,k}|_t - E_y^{i,j,k}|_t}{\Delta x} - \frac{E_x^{i,j+1,k}|_t - E_x^{i,j,k}|_t}{\Delta y} = -\frac{\mu_{zz}^{i,j,k}}{c_0}\frac{\widetilde{H}_z^{i,j,k}|_{t+\frac{\Delta t}{2}} - \widetilde{H}_z^{i,j,k}|_{t-\frac{\Delta t}{2}}}{\Delta t}$$

$$\frac{\widetilde{H}_z^{i,j,k}|_{t+\frac{\Delta t}{2}} - \widetilde{H}_z^{i,j-1,k}|_{t+\frac{\Delta t}{2}}}{\Delta y} - \frac{\widetilde{H}_y^{i,j,k}|_{t+\frac{\Delta t}{2}} - \widetilde{H}_y^{i,j,k-1}|_{t+\frac{\Delta t}{2}}}{\Delta z} = \frac{\epsilon_{xx}^{i,j,k}}{c_0}\frac{E_x^{i,j,k}|_{t+\Delta t} - E_x^{i,j,k}|_t}{\Delta t}$$

$$\frac{\widetilde{H}_x^{i,j,k}|_{t+\frac{\Delta t}{2}} - \widetilde{H}_x^{i,j,k-1}|_{t+\frac{\Delta t}{2}}}{\Delta z} - \frac{\widetilde{H}_z^{i,j,k}|_{t+\frac{\Delta t}{2}} - \widetilde{H}_z^{i-1,j,k}|_{t+\frac{\Delta t}{2}}}{\Delta x} = \frac{\epsilon_{yy}^{i,j,k}}{c_0}\frac{E_y^{i,j,k}|_{t+\Delta t} - E_y^{i,j,k}|_t}{\Delta t}$$

$$\frac{\widetilde{H}_y^{i,j,k}|_{t+\frac{\Delta t}{2}} - \widetilde{H}_y^{i-1,j,k}|_{t+\frac{\Delta t}{2}}}{\Delta x} - \frac{\widetilde{H}_x^{i,j,k}|_{t+\frac{\Delta t}{2}} - \widetilde{H}_x^{i,j-1,k}|_{t+\frac{\Delta t}{2}}}{\Delta y} = \frac{\epsilon_{zz}^{i,j,k}}{c_0}\frac{E_z^{i,j,k}|_{t+\Delta t} - E_z^{i,j,k}|_t}{\Delta t}$$

Note that every equation contains a term on the right side that describes a unique field component quantity at the "next" time step. By trivially rearranging these equations, one can derive the update equations for all electric and magnetic field components.

Total Field/Scatter Field (TF/SF).

In FDTD programs, the simulation grid is typically split into two regions: the total field region where field quantities from sources and scattering objects are simulated and the scatter field region where only field quantities scattered from an object are simulated. This allows the user to record only the energy scattered off an object of interest at some point. Implementing a TF/SF has the added benefit of introducing one-way plane wave sources.

The general technique for implementing a TF/SF is to analyze the update equations and note the curl terms require field quantities from an adjacent cell. At the boundary of the TF/SF, these terms would contain quantities from the total field side in updates at a scatter field point and vice-versa for updates at a total field point. To correct these terms, one simply subtracts the source function from total field quantities (thereby making the term a scatter field quantity) and adds the source function to scatter field quantities (thereby making them total field quantities).

The source function is defined by the programmer in the form of a time array spanning the simulation's duration. The programmer must define a source for both electric and magnetic fields as the magnetic field is staggard by a half grid cell and half time step. The user must also scale one of the fields by multiplying with the free space impedance.

In practice, implementation requires the programmer to do a standard update of the curl terms across the grid, then correct the terms at the boundaries of the TF/SF regions by adding or subtracting source terms.

Perfectly Matched Layers (PML).

The perfectly matched layer is a region of the grid at the outer edges modified such that waves entering at any given angle of incidence, polarization, and frequency will rapidly decay to zero with minimal reflections. They are thus a method of terminating waves that are exiting the simulated region without causing further interactions.

To accomplish this, loss is introduced in the PML regions. Since loss contributes to reflections, the impedance must be matched through the complex permittivity to compensate. Furthermore, the PML must work for all angles of incidence, frequencies, and polarizations. Therefore, the permittivity and permeability values in the PMLs must be

made anisotropic. Since this is all done using Maxwell's equations in the frequency domain, Fourier transforms are used to return to the time domain. Finally, since the Fourier transforms result in partial derivatives and integrals, finite difference approximations are used to derive a new set of update equations.

While a thorough derivation of the update equations with PMLs is beyond the scope of this report, an excellent resource for further research are lectures 3c and 3d from Dr. Raymond Rumpf referenced below.

Additional Features.

The Courant Stability Condition

The Courant Stability Condition is a necessary condition for convergence of numerical PDE solutions. The condition requires the integration time step to be such that the wave simulated does not travel further than one grid cell. That is,

$$\frac{c_0}{\eta}\Delta t < \Delta x$$

More generally,

$$\Delta t < \frac{\eta}{c_0\sqrt{\frac{1}{(\Delta x)^2}+\frac{1}{(\Delta y)^2}+\frac{1}{(\Delta z)^2}}}$$

Boundary Conditions

With the use of PMLs surrounding the grid, Dirichlet[2] boundary conditions are typically used at the grid edges. This way, any waves entering the PMLs will decay rapidly before reflecting off the edges and traveling through the PML a second time.

---

[2] Dirichlet boundaries simply set the field at the boundary to zero. This in effect creates a PEC and causes any incident waves to reflect completely.

To set boundary conditions, the curl terms requiring field quantities from outside the grid are corrected explicitly outside the main spatial loops used to calculate the curl. The programmer simply sets the offending terms to zero.

Source Functions

Source functions are defined such that the sources "turn on" slowly following a short buffer period after the simulation begins. This way, numerical dispersion is not introduced due to sudden changes in the electric and magnetic field quantities. Typical sources used include Gaussians and sinusoids.

Modelling Metals

Metals are generally modelled in one of four ways:

1. Setting the dielectric constant to an arbitrarily high value,
2. Using an auxiliary array to set grid points to be perfect electric conductors,
3. Introducing currents through Ampere's Law,
4. Using a Lorentz-Drude Model.

These methods consecutively increase in complexity. In the case of this project, a PEC array is likely sufficient.

Implementation of FDTD in EMITRACK

This section first details any approximations made prior to modeling, then describes the implementation of FDTD in order of appearance in the EMITRACK 2D_FDTD_TM_PML.py program. The implementation in 2D_FDTD_TE_PML.py falls in analogy. Any significant changes between the two are noted below. Note that this section is intended to be supplemental to comments in the aforementioned python programs.

This project approximates the overdense meteor trail as a metallic cylinder of infinite height. Therefore, any changes along the z-axis of the cylinder (i.e. $\frac{\partial}{\partial z}$) are zero. This is referred to as a 2D FDTD simulation and was used for the final model. The resulting update equations after cancellations are then split into two modes: the transverse electric (TE) mode describing electric field components in the x-y plane, and the transverse magnetic (TM) mode describing the electric field component along the z-axis of the cylinder. Each mode contains a set of coupled update equations describing three of the six field components.

Import Statements.

The programs use standard python libraries "NumPy" for arrays; math functions; and other utilities, and "Matplotlib" for plotting. "time" is imported to time program execution to quantify optimization improvements. "Numba" is a python optimization library from which the "just-in-time" function wrapper is imported. This is used to compile the main FDTD loop into machine code which significantly improves program performance. "MoviePy" is a python library used to generate animations from matplotlib plots.

Radar Params.

The "radar params" section defines the central frequency and pulse width of the source used in the simulation. The source itself is defined further on.

Computing Grid Resolution.

Grid resolution in FDTD is determined by the wavelength and the scattering object's smallest structure. Since the object in question is a cylinder and therefore has no "smallest structure", only the wavelength is used to determine grid resolution. The minimum wavelength in the grid is calculated and resolved with 20 grid cells by default.

Building Grid.

Grid size is selected arbitrarily with consideration to the scattering object size and wavelengths used. A 2x grid is defined only to set PEC, permittivity, and permeability values across the grid. The scattering cylinder is built by iterating over the grid and setting locations within the cylinder radius about the cylinder location to be zeros in the PEC array. The remaining values in the PEC array are ones.

Time Params, Pulse Params, and Iteration Number Calculation.

The time increment is defined using the Courant stability condition. Pulse params are used to define properties of a gaussian source. This was originally used as the primary source, but now serves to shape the sinusoidal source. The number of iterations is determined by calculating the total time for the source to turn on and off with some delay and for the waves to propagate across the grid five times. The user is prompted to keep or override this number.

Source Functions (TF/SF).

The time array, source position, magnetic field source offset, and magnetic field source scale are defined. Source shape arrays are defined using a gaussian to initiate the source, pulse width to maintain the source at max amplitude, and a second gaussian to terminate the source. Source arrays are then defined as cosine function time arrays multiplied by the shaping arrays.

PML Parameters.

PML arrays are defined as 2D arrays spanning the 2x grid filled with zeros. Using the PML sizes defined when building the grid, a cubic function is used to ramp the PML

array values from zero to one. Note that by setting the PML arrays to zero, the PMLs may be “turned off”.

Update Coefficients and Initializations.

All update coefficients are defined such that the update equations include only additions and multiplications. The fields, curls, and integrals used in the program are initialized. 3-dimension arrays are defined to store electric field components every tenth iteration. These arrays use single float precision as they are only used in animations.

Main FDTD Loop.

The main FDTD loop is defined as a function solely for use with the Numba JIT function wrapper. Within the function, a loop iterates over time. The curl arrays used in the magnetic field update equations are updated with care taken to appropriately calculate the curl at boundaries. The electric field source is introduced in the curl update. The respective integrations are then updated. Next, the magnetic fields are updated. Note that the magnetic field update position in the time loop implicitly defines it to be staggard a half time-step from the electric field update. A similar procedure then occurs for the electric field update: curl equation updates, source injection, integral updates, then field updates. Finally, the electric field is stored in the 3-D storage array. The sum of the electric field is calculated across a slice located behind the source.

Plotting, Storage, and Preview Animation.

The magnitude of the electric field received is plotted as a function of time. The sum of the absolute value of the received energy is also calculated and presented on the plot. The figure is then saved.

The electric field time array and relevant parameters are saved to drive as ".npy" files. A short preview animation is then generated showing the electric field every 50th time-step.

EMITRACK Output Testing

Due to the lack of complete TF/SF implementation, plasma simulation, and a near-field to far-field transform, this program is likely not sufficient to accurately model the relevant interaction. Therefore, this section will focus primarily on a battery of tests conducted to determine the validity of the program in its current state. These are basic tests whose results can easily be verified and cross-referenced with well-understood phenomena or traced back to isolate and correct areas of issue in the program. The results of these tests are listed in the order of appearance in the results section below.

Source Testing.

The first few tests determine the validity of source functions.

Zero Sources

The first test simply ensures no undesired sources are present in the program and ensures no other components introduce energy. This is done by setting all source functions to zero. The lack of sources should result in zero fields everywhere in the grid for the duration of the simulation.

Source Profile

UAF meteor radars use a shaped amplitude profile with a carrier frequency of 32.55 MHz. The pulse has a width of 5 μs with the endpoints rounded off to ease in/out of the source without adverse effects due to mismatched phase. To verify this profile is modelled correctly, the source functions are plotted as a function of time. The expected profile should

be a cosine curve whose amplitude gradually increases to a maximum, maintains the maximum for some time, then decays to zero.

Source Introduction

To ensure the source is introduced correctly, all update equations are turned off by commenting out all curl terms. This way, the only changes to the fields are from direct injection of the source function. The expected result is sharp sinusoidal oscillations at the location where the source is injected. Otherwise, the grid should remain undisturbed since the update equations are off.

Update Equations Testing.

The update equations make the core of any FDTD program; therefore, care must be taken to ensure they are implemented correctly. Their validity can be partially tested through verifying conservation of energy and direct observations in intuitive cases.

Conservation of Energy.

The laws of physics dictate that energy may not be created or destroyed. This must hold true in any physics simulation to within numerical uncertainty. To verify conservation of energy, the magnitude of the electric field about the source introduction is integrated over position and time. Then the magnitude of the electric field exterior to the source position and surrounding the grid near the edges is integrated over position and time. Since the source function describes energy going into the grid and the magnitude of the electric field at the edges describes energy moving out of the grid, the sum of the quantities should match. This method was implemented with a point source at the center of the grid.

Reflections and Interference.

While the results of most FDTD simulations are difficult to certify as "correct", some simple simulations can be run to verify that the program is not obviously wrong. FDTD models EM waves and EM waves are known to interfere constructively and destructively. EM waves are also known to have an angle of reflection equal to the angle of incidence. Therefore, by placing a source in an empty grid with Dirichlet boundaries and observing the behavior of the waves in such a controlled manner, the appropriate interference and reflections should be clearly visible.

PML Testing.

The perfectly matched layer boundary regions bordering the grid are designed to rapidly decay any waves propagating through them. They are, however, not perfect. Any waves entering the PMLs reflect small amounts of radiation back into the grid. This reflection is measurable and therefore its magnitude should be recorded and considered.

PML Function Check

Before measuring any reflection, a test to ensure PML function is conducted. By placing a source at the center of the grid and measuring the integral of the magnitude of the electric field interior to the PMLs as a function of time, the integral should drop to approximately zero (excluding PML reflections) after the source, characterized by a clear spike in energy, passes through.

PML Reflection Measurement

PML reflections can be measured by comparison. First, a simulation is run without PMLs. A source is introduced at the center of the grid. The total radiation from the source is measured as it passes through a boundary interior to the PML. The simulation is timed

such that the waves do not propagate back through the measurement boundary. Then, the same test is performed with PMLs. By subtracting the total radiation without PMLs from with PMLs, the radiation from PML reflections can be calculated.

Results

To reiterate, the results presented are a set of tests run to determine the validity of the program's output.

Source Testing

Zero Sources.

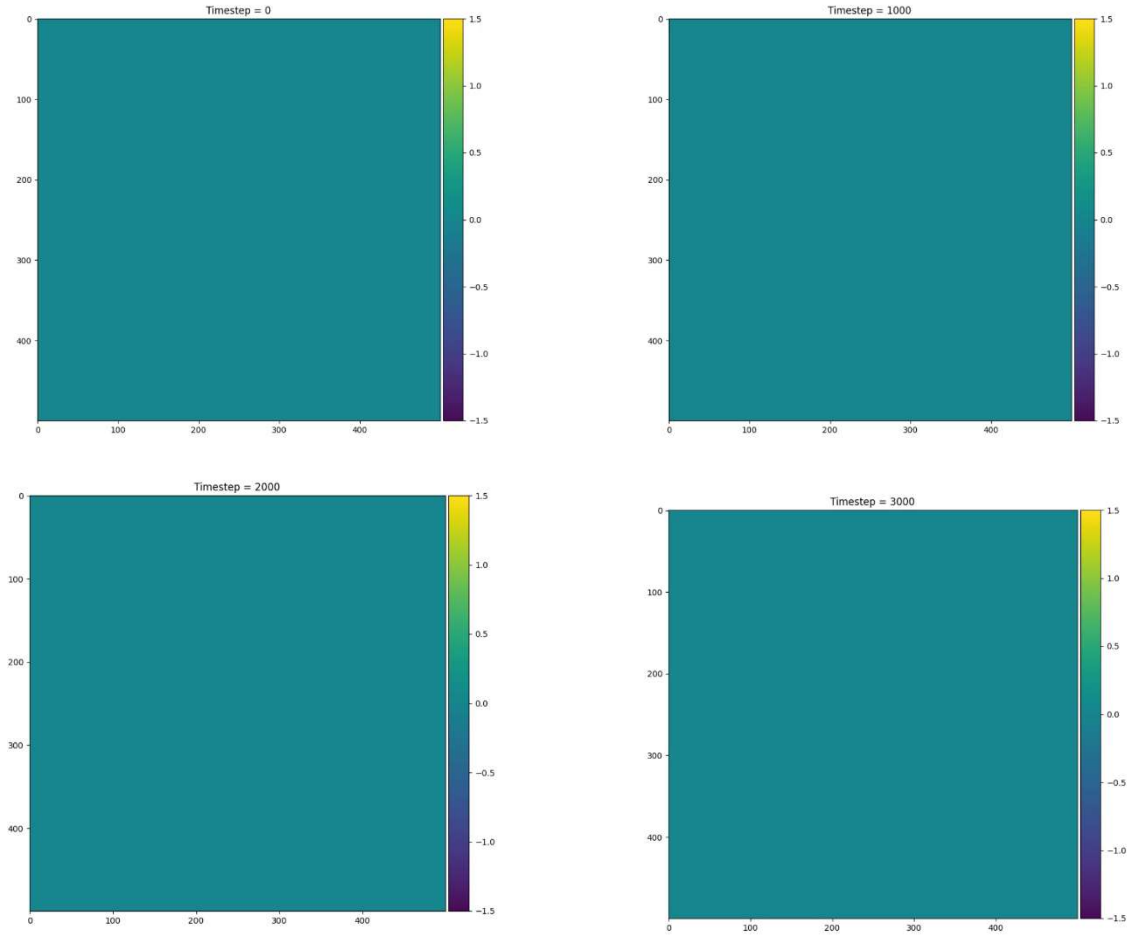

Figure 2. The lack of sources results in zero electric fields across the grid.

Source Profile.

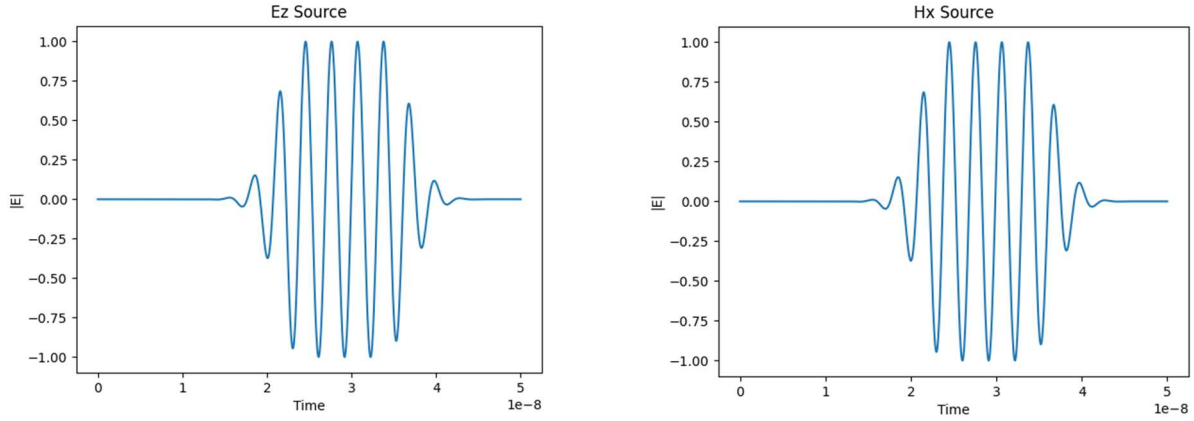

Figure 3. The profile of the source as a function of time is similar to the UAF PFRR meteor radar pulse.

Source Introduction.

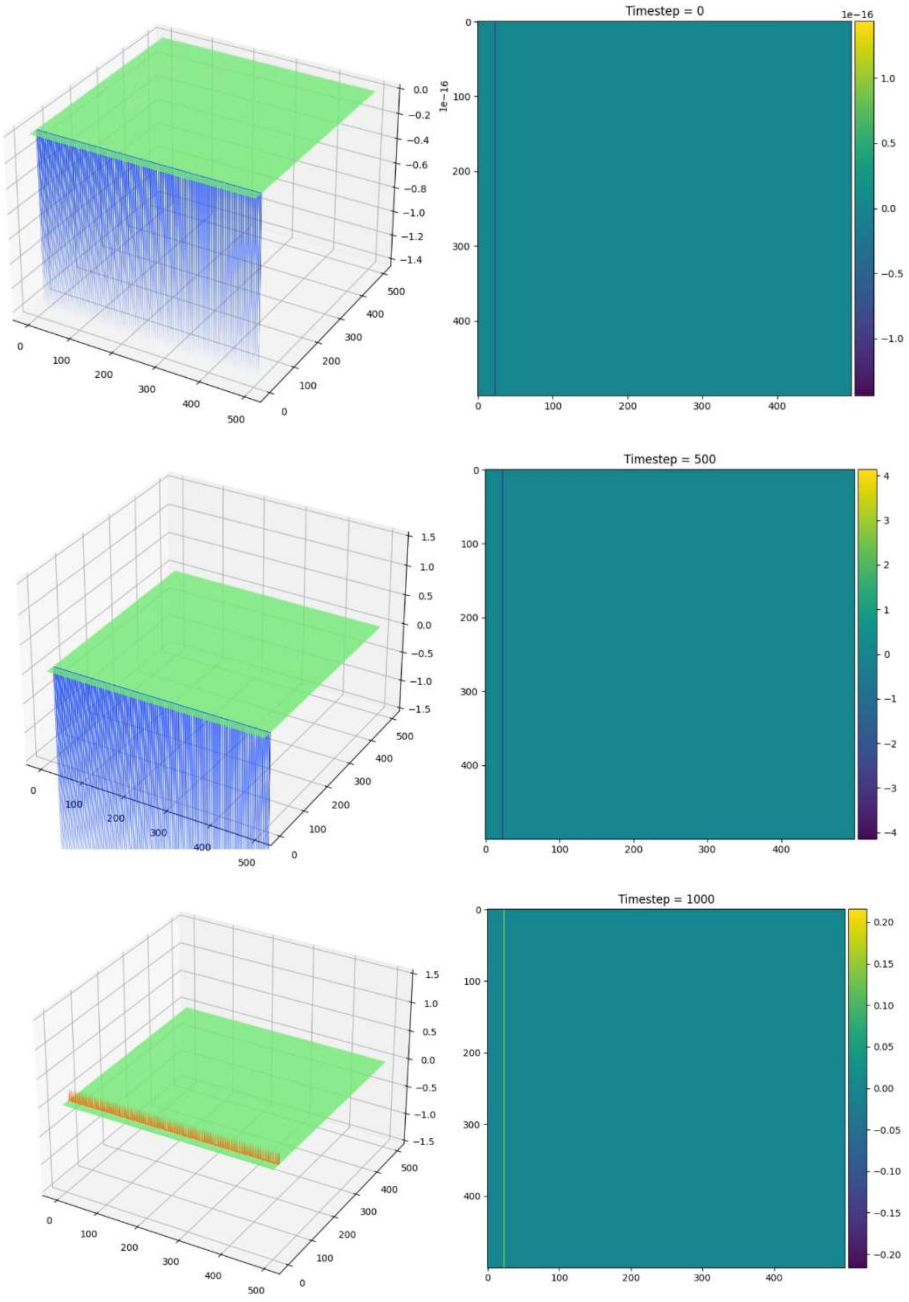

Figure 4. The pulse is introduced in the appropriate position.

Update Equations Testing

Conservation of Energy.

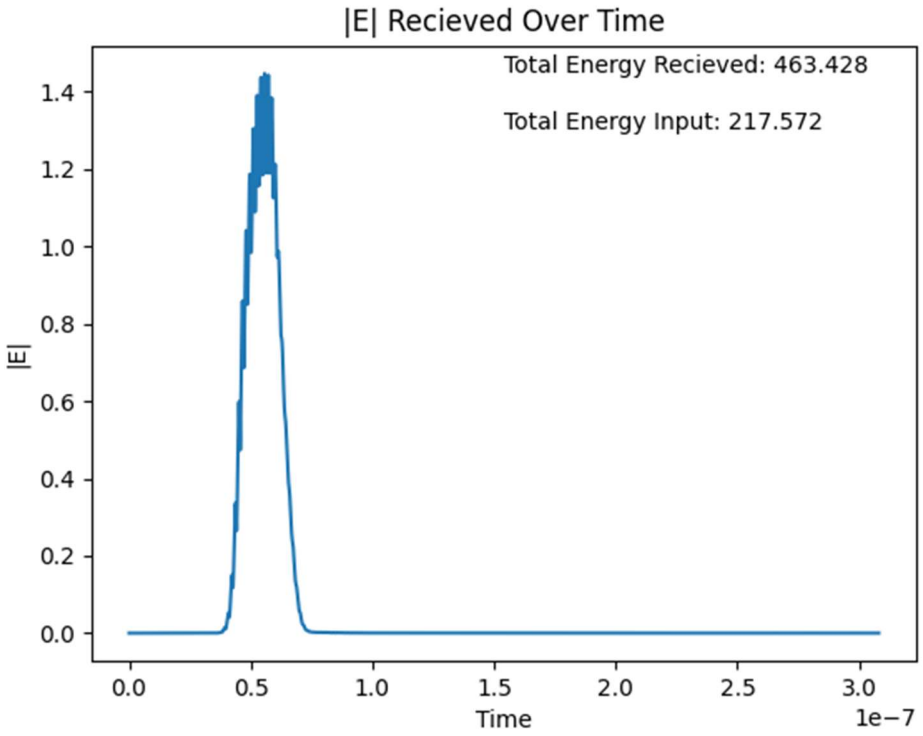

Figure 5. The plot of the sum of the magnitude of the electric field around the edges of the grid shows the total outgoing energy to be higher than the input energy.

Reflections and Interference.

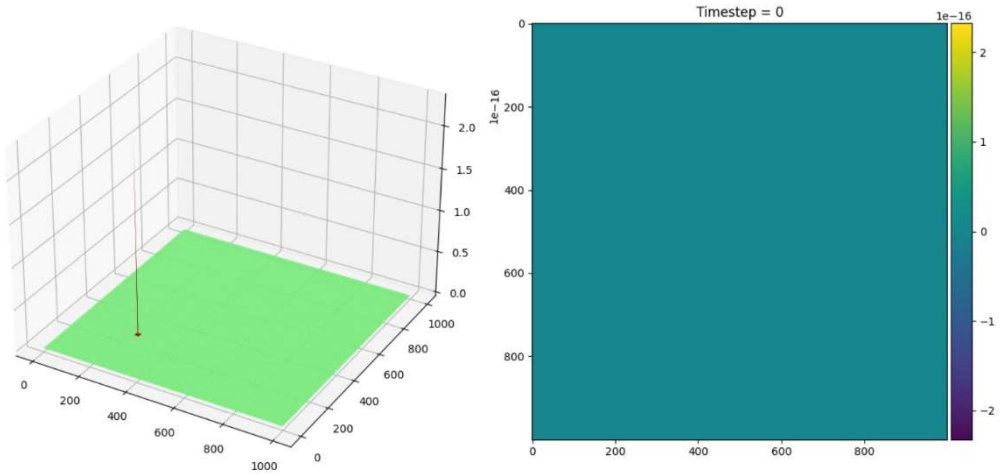

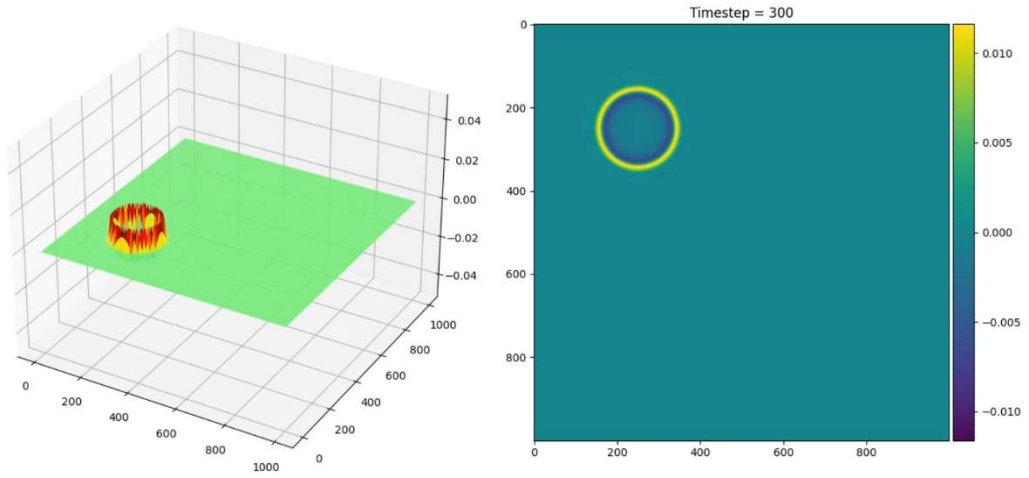
Timestep = 300

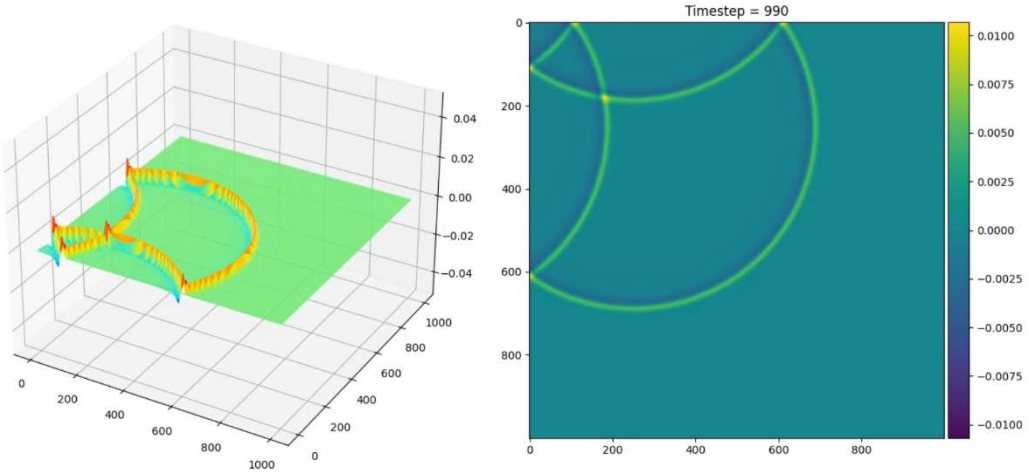
Timestep = 990

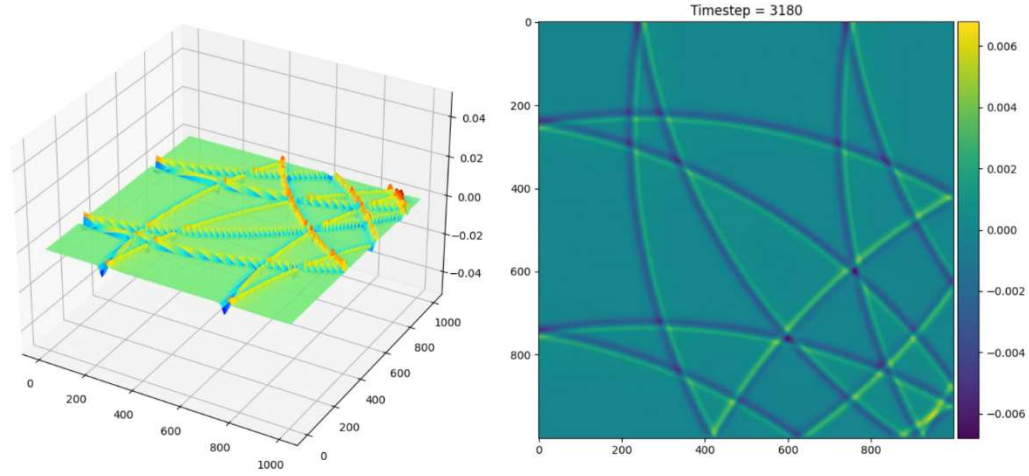
Timestep = 3180

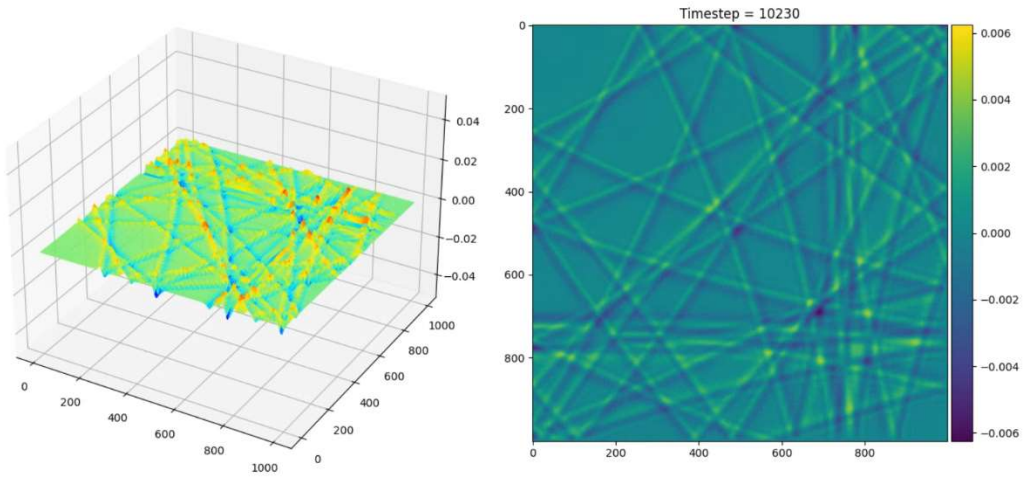

Figure 6. The electric field is introduced, radiates outward, reflects off Dirichlet boundaries, and experiences interference.

PML Testing

Due to the failure of the methodology to measure conservation of energy, PML testing was not conducted due to the two tests sharing the same methods.

Discussion

Results

Source Testing.

Source testing showed promising results. No unwanted sources appeared due to some issue with update equations, the source followed the appropriate profile similar to the UAF PFRR meteor radars, and the source was introduced in the appropriate position in the grid.

Update Equations Testing.

The methodology used to verify conservation of energy appears to be flawed. By plotting the fields as a function of time, nearly all energy within the grid appears to decay due to radial expansion and exit the grid as expected. This result does not appear to be replicated in the calculation of total energy leaving the grid versus energy entering the grid.

The total energy input was 217.572 units. The energy output was 463.428 units, nearly double the input. Further study must be conducted to determine the cause of this discrepancy. The implementation of other more common methods used to verify conservation of energy, such as frequency transmittance and reflectance measurement, would likely be a good option.

Reflections and interference appeared as expected. Waves incident on boundaries reflected at their angle of incidence and constructive/destructive interference occurred where waves intersected.

PML Testing.

Since the methods used to verify conservation of energy are also implemented to determine PML behavior, PML testing was omitted due to the failures in the conservation of energy tests.

Further Development

Two notable features missing from this program are complete TF/SF implementation and near-field to far-field transforms. Implementation details for both items can be found in lecture 5b from Dr. Rumpf. It may also prove necessary to implement a plasma model, which is detailed in (Sullivan & Houle, 2020).

TF/SF Implementation.

The complete total field/scatter field implementation requires the programmer to implement TF/SF boundaries about the grid. In practice, this requires all curl terms to be corrected with appropriate source terms in analogy to the current implementation. The source terms must then be derived. This requires the programmer to consider the wave vector and the components of the fields incident on each boundary.

Near-Field to Far-Field Transform.

The near-field to far-field transform is a method of simulating EM waves travelling very long distances prior to measurement. These distances are far too great to simulate in their entirety in a practical manner, therefore the transform allows programmers to simulate the far-field response of scattering objects within reasonable time constraints. Since the meteor trails being simulated are at altitudes of the order of tens of kilometers and since the grid is by default discretized with 0.05 m spatial increments, the near-field to far-field transform is required to fully simulate the interaction.

Plasma Model.

Plasma can be modelled in a FDTD simulation through the permeability. Given a plasma number density, one can derive an expression for the permeability of such a plasma. This is a complex expression which will require Z-transforms and Fourier transforms to reduce to an implementable form.

Conclusion

In its current state, EMITRACK is an FDTD program capable of simulating objects of finite extent in two dimensions. The code is split into two programs: one for the TM mode describing waves polarized along the z-axis and one for the TE mode describing waves polarized along the x-axis. The programs are configured for the case of a PEC cylinder of infinite height along the z-axis. The simulations include a TFSF boundary implemented along one side of the grid with source functions generating a sinusoidal oscillation with a gaussian shaped amplitude. The simulation grid is surrounded by perfectly matched layers; a region where entering waves decay rapidly to zero with minimal reflections independent of incidence angle, polarization, and frequency. As a simulation is run, the sum of the electric field magnitude across a slice of the grid

between the PML and TFSF boundary is recorded. This represents the energy return from the scattering cylinder. EMITRACK has undergone function and validity testing to determine its ability to represent real world phenomena. This testing returned reasonable results; however, the program is limited in its function due to lack of features. Further development and testing is required to accurately model the relevant phenomena.

The UAF PFRR meteor radars detected unexpected oscillations in the return signal from overdense meteor trails. While incomplete, EMITRACK does provide a foundation for simulation of the meteor scattering phenomena. The radar parameters are known and implemented and the overdense meteor is approximated as a PEC cylinder. Future researchers need to implement a near-field to far-field transform and a TFSF surrounding the grid. This should prove sufficient to accurately model the phenomena and provide results. Next, thorough testing is required to verify results. Should the results prove unreasonable, a plasma model may be required to better define the meteor trail. Introductions and relevant sources to implement these features have been included in the future development section above. The EMITRACK program can be found on GitHub at https://github.com/Raptor287/EMITRACK.

References

Baggaley, W. J., & Fisher, G. W. (1978, October). Measurements of the Initial Radii of the Ionization Columns of Bright Meteors. *Planetary and Space Science, 26*(10), 969-977.

Manning, L., Villard, O., & Peterson, A. (1952, August). The length of ionized meteor trails. *Transactions of the IRE Professional Group on Antennas and Propagation, PGAP-3*, 230-230. doi:10.1109/T-AP.1952.28044

Richardson, J., & Bedient, J. (n.d.). *Meteor FAQs*. Retrieved from American Meteor Society: https://www.amsmeteors.org/meteor-showers/meteor-faq/

Rumpf, R. C. (n.d.). *Electromagnetic Analysis Using Finite-Difference Time-Domain*. Retrieved from EMPossible: https://empossible.net/academics/emp5304/

Sevgi, L. (2003). *Complex Electromagnetic Problems and Numerical Approaches.* Piscataway: IEEE Press.

Sullivan, D. M., & Houle, J. E. (2020). *Electromagnetic Simulation Using The FDTD Method with Python.* Wiley-IEEE Press.

Taflove, A., & Hagness, S. C. (2005). *Computational Electrodynamics: The Finite-Difference Time-Domain Method.* Norwood: Artech House.

Understanding the Finite-Difference Time-Domain Method, John B.

Schneider, www.eecs.wsu.edu/~schneidj/ufdtd, 2010.

Wikipedia. (2022, October 23). *Finite-difference time-domain method*. Retrieved from Wikipedia: https://en.wikipedia.org/wiki/Finite-difference_time-domain_method

Wislez, J. -M. (1996). Forward scattering of radio waves off meteor trails. *International Meteor Conference*, (pp. 99-117). Brandenburg, Germany. Retrieved from

https://www.researchgate.net/publication/234500894_Forward_scattering_of_radio_waves_off_meteor_trails

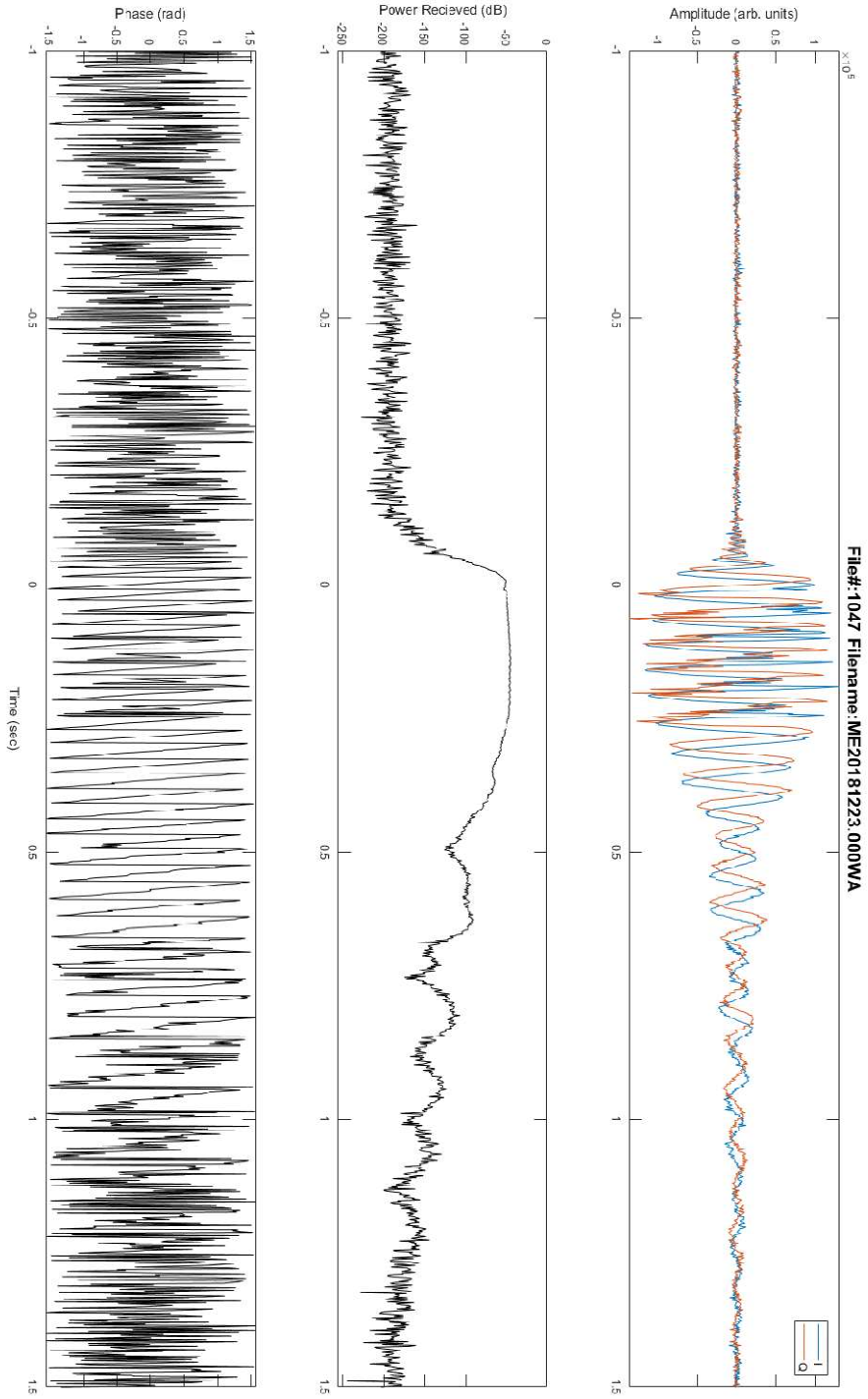

Figure 7. The radar return from an overdense meteor trail shows unexpected oscillations in the decay scheme.